The spectral scale of surface wave breaking

Johannes Gemmrich, University of Victoria, Victoria, BC, Canada
gemmrich@uvic.ca

Surface waves have been labeled the gearbox between atmosphere and ocean (*Ardhuin, et al.*, 2005), and in particular, wave breaking plays an important role in many air-sea exchange processes. At moderate to high wind speed the momentum transfer from wind to ocean currents passes through the wave field via wave breaking. The breaking of surface waves is responsible for the dissipation of wave energy, yielding enhanced turbulence kinetic energy (TKE) levels in the near-surface layer and to play an important role in upper ocean processes. Breaking waves not only transfer energy, momentum heat and gases from the atmosphere to the ocean surface layer but also enhance aerosol generation and latent heat fluxes due to sea spray. Breaking waves also disperse pollutants and generate underwater sound. Furthermore, wave breaking affects wave development as it dominates the dissipation of wave energy and controls wave growth. To improve our understanding of wave-breaking related processes a twofold approach is necessary: i) detailed process studies e.g. energy dissipation, mixing, sound generation, etc. and ii) knowledge of the occurrence and scale of wave breaking. Here we focus on the latter.

It is well known even to the casual observer that wave breaking occurs at a wide range of scales. This breaking scale is of great importance to all physical processes associated with wave breaking. For example, a small scale breaker dissipates less energy than a breaking dominant wave. Therefore, we are interested in breaking probabilities of different wave scales.

$$P(c) = \frac{N_{brk}(c, c+\Delta c)}{N_{all}(c, c+\Delta c)}, \qquad (1)$$

where N_{brk} is the number of *breaking wave crests* propagating with velocities in the range $(c, c+\Delta c)$ passing a fixed point and N_{all} is the total number of *wave crests* propagating with velocities in the range $(c, c+\Delta c)$ passing a fixed point. *Banner et al.* (2002) found that the breaking probability increased roughly linearly with wave saturation.

Defining multiscale breaking probabilities by equation (1) requires the knowledge of the total number N_{all} of wave crests of a certain scale passing a fixed point. However, this measurement is commonly not available, and in a directional (short crested) wave field not readily defined. A more practical measure was introduced by *Phillips* (1985). Realizing that the scale of a breaking wave may be defined by the length of the breaking crest and its propagation speed, he defined $\Lambda(c)$, the spectral density of breaking wave crest length per unit area and velocities in the range $(c, c+\Delta c)$. So far, observations of $\Lambda(c)$ are limited (*Phillips et al.*, 2001; *Melville and Matusov,* 2002).

The passage rate of breaking crests propagating at speed c past a fixed point is $c\Lambda(c)$. As breaking crests propagate they turn over a fraction of the sea surface. The fractional surface turnover rate per unit time is

$$R = \int c\Lambda(c)dc \qquad (2)$$

which can also be interpreted as the breaking frequency at a fixed point $\tilde{P}_{brk} = R$ (*Phillips,* 1985).

Towed hydrofoil experiments (*Duncan,* 1981) established the rate of energy loss per unit length of breaking crest to be proportional to c^5, where c is the crest propagation speed. Therefore, the fourth and fifth moment of $\Lambda(c)$ are related to the dynamics of wave breaking. The wave energy dissipation due to the breaking of waves of scale corresponding to phase speed c is

$$\varepsilon(c)\,dc = b\rho g^{-1}c^5\Lambda(c)\,dc \qquad (3)$$

where b is an unknown, nondimensional proportionality factor, assumed to be constant (*Phillips,* 1985).

The total energy dissipation associated with whitecapping is

$$E = b\rho g^{-1}\int c^5\Lambda(c)dc \qquad (4)$$

The spectrally resolved momentum flux from breaking waves to currents is

$$m(c)\,dc = b\rho g^{-1}c^4\Lambda(c)\,dc\,, \qquad (5)$$

yielding a total momentum flux from the wave field to currents

$$M = b\rho g^{-1}\int c^4\Lambda(c)dc\,. \qquad (6)$$

However, it should be stressed that any quantitative assessments of energy dissipation and momentum fluxes directly depend on the proportionality factor *b,* and therefore require a thorough understanding of its value and functional behaviour.

Although this theoretical framework of energy dissipation based on breaking crest distributions has been developed two decades ago, observations of $\Lambda(c)$ in the ocean are still very limited (Ding & Farmer, 1994, Phillips et al., 2001, Melville & Matusov, 2002) and are inconclusive.

Observations

We describe observations of breaking crest distributions in the open ocean at wind speeds of 10 – 12 m/s and examine the implied energy dissipation, momentum flux and breaking frequency.

Observations of the surface wave field were taken as part of the FAIRS (Fluxes, Air-sea Interaction and Remote Sensing) experiment aboard the research platform *FLIP* in the open ocean 150 km offshore of the central Californian coast (Gemmrich & Farmer, 2004). Two analog black/white video cameras mounted on *R/P FLIP* yielded recordings of the ocean surface with overlapping fields of view of 15.4 x 20.5 m (Camera 1) and 9 x 12 m (Camera 2).

The video recordings were digitized at 640 x 480 pixels, ensuring that even the smallest visible whitecaps were resolved. Differential images were generated by subtracting successive video frames. These images highlight propagating breaking crests and filter out all stationary signals including foam. An image processing scheme approximates the identified breaking crests as ellipses, and their major axes define half the length of the breaking crest $L_{br}/2$. Displacement of the ellipse's centroid yields the raw propagation speed of the breaking crest $\tilde{c}_{br}$. Subtracting the potential advection by the orbital motion of underlying longer waves u_{orb} yields the true breaker speed $c_{br} = \tilde{c}_{br} - u_{orb}$. The equivalent linear phase speed c of

the wave associated with the breaking crest is somewhat larger (Melville & Matusov, 2002); here we take $c = c_{br} / 0.85$.

The FAIRS experiment included wind conditions ranging from almost calm up to 15 m/s. The resulting wave field ranged from purely swell conditions with significant wave height $H_s < 1\text{m}$ to young wind seas on top of swell with $H_s > 4\text{m}$. Here we report on four fetch-unlimited data sets recorded under various wind forcing and wave field conditions.

Data set I, September 29, 2000, 0950 to 1450UTC follows a period of increasing wind speed. For several days prior to this data set winds were very light (<4 m/s) and the wave field was dominated by swell with $H_s < 1\text{m}$. Approximately 11 hours before the start of this data set the wind speed u_{10} increased steadily for a period of 10 hours and peaked at $u_{10} = 12.8\,\text{ms}^{-1}$. Throughout the data set the wind speed stayed nearly constant at 12m/s. At the beginning of the data set the significant wave height had increased to $H_s = 2.8\text{m}$ and continued to rise to 3.1m. The dominant wave period was $f_p = 0.13\,\text{Hz}$ and the wave age $c_p/u^* \approx 26$, where c_p is the phase speed of the dominant waves and u_* is the friction velocity in air. This data set represents a *developing sea*.

Data set II on October 3, 0005 UTC – 0230 UTC occurred after three days of sustained wind speed u_{10} > 10 m/s with well developed wind waves at wave age $c_p/u^* \approx 34$, significant wave height $H_s = 3\,\text{m}$ and dominant frequency $f_p = 0.11\,\text{Hz}$. The wind speed was $u_{10} \approx$ 11.5 m/s. This data set represents a *developed sea*.

The third data set, October 3, 2345 UTC – October 4, 0245 UTC, represents a *fully developed sea*. The dominant frequency remained unchanged at $f_p = 0.1\,\text{Hz}$, the wind speed has increased to $u_{10} \approx$ 12.5 m/s and the significant wave height reached $H_s = 3.2\,\text{m}$ at a wave age $c_p/u^* \approx 36$.

Data set IV on October 10, 1100 - 1430 UTC occurred at the end of a rapid increase of wind speed from <5m/s to ≈13m/s. The significant wave height increased from <2m to >4m. The data set itself covers the period of slow increase in wind speed, from 11.8 m/s to 13 m/s, but a significant increase in wave height from $H_s = 2.5\,\text{m}$ to $H_s = 3.9\,\text{m}$ and reduction in dominant wave frequency from $f_p = 0.16\,\text{Hz}$ to $f_p = 0.1\,\text{Hz}$. The wave age was $c_p/u^* \approx 35$. This data set represents a growing sea superimposed onto significant swell and will be labeled *mixed sea.*

Scale of breaking waves

Our analysis extracts the phase speed c_{br} of every breaking event occurring within the video footprint during the observation period. Normalization of the breaking wave phase speed by the dominant phase speed c_{br} / c_p yields information on the spectral occurrence of wave breaking.

Wave breaking occurs over a wide range of scales (Figure 1, Figure 2). However, the breaking scales cover different ranges of the wave spectrum, depending on wave development. In the

young sea case, phase speeds of breaking waves range from roughly 1/10 of the dominant phase speed (*i.e.* with a wavelength corresponding to 1/100 of the dominant wavelength) up to the dominant waves. In contrast, in a fully developed sea we observed hardly any breaking at scales corresponding to phase speeds larger than about $0.4\,c_p$. As the wave age increases, the distribution of breaking scales narrows significantly and the peak of the breaker phase speed distribution shifts from about $0.4\,c_p$ to $0.2\,c_p$.

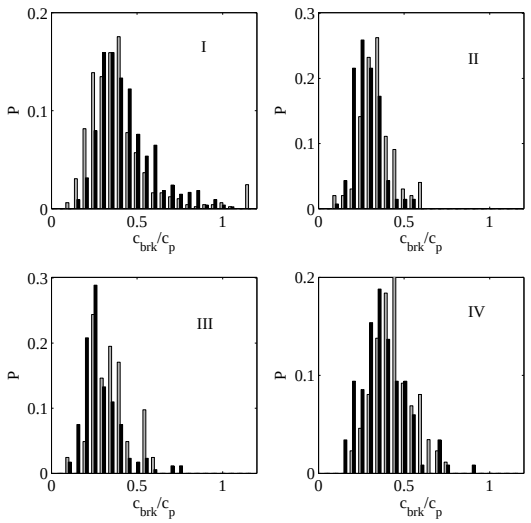

Figure 1: Distribution of the normalized whitecap propagation speed c_{brk}/c_p as obtained from Camera 1 (gray bars) and Camera 2 (black bars). The four data sets described in the text are indicated by I – IV.

Breaking crest length distribution *Λ(c)*

For each breaking event the whitecap propagation speed c_{br}, the length of the major object axis L_{br} and the event duration t_{br} are known. At an arbitrary instant during the total observation period *T*, the expected breaking crest length of an individual event is $L_{br}\,t_{br}/T$. The expected breaking crest length of an event in the speed range $c, c+\Delta c$ is the summation over all events which are within this speed range, $\sum L_{br}\,t_{br}/T$. Thus, the average length of breaking crest per unit area per unit speed interval $\Lambda(c)\,dc = \sum L_{br}\,t_{br}/(T\,A)$, where A is the area of the video footprint and the results are transformed to linear phase speed dependence.

The breaking crest length distribution $\Lambda(c)$ shows a slightly different behaviour than the breaking occurrence rates given in Figure 1. For the following analysis, data set I, which occurred during a period of rapid wave field development, has been divided into two segment of equal number of whitecap events.

For all five data segments, $\Lambda(c)$ peaks at intermediate wave scales with phase speeds of 3 – 4 ms^{-1}, corresponding to $c/c_p \approx 0.3$ (Figure 2). In the peak region, $\Lambda(c)$ values of the different data sets vary by roughly a factor two, whereas at the smallest and the largest wave scales the different data sets spread more than one order of magnitude. Melville and Matusov (2002) found a scaling factor $(10/u_{10})^3$, where u_{10} is the 10 m height wind speed value in ms^{-1}, to collapse their data sets recorded at average wind speeds between 7.2 ms^{-1} and 13.6 ms^{-1}. For our four data sets this scaling factor varies by less than 15% and therefore does not significantly reduce the spreading between $\Lambda(c)$ values of the different data set. Furthermore, we do not expect that a physically arbitrary scaling factor would be universally applicable.

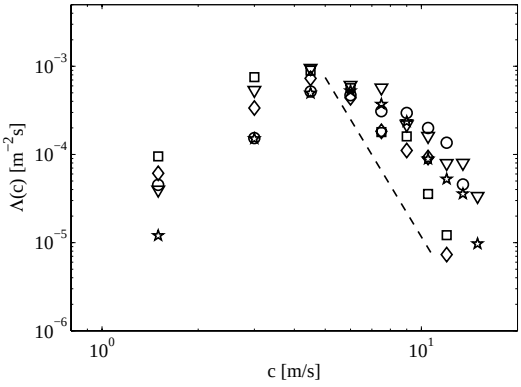

Figure 2: Breaking crest length per unit area $\Lambda(c)$ as function of the breaking wave phase speed c. The symbols (○,▽,□,◊,⋆) correspond to data sets (Ia, Ib, II, III, IV), respectively. The dashed line indicates a c^{-6}-dependence, predicted in Phillips (1985).

Momentum flux and energy dissipation due to breaking are given by the fourth and fifth moment of the breaking crest length distribution. These higher moments are weighted towards larger wave scales (larger c). However, the proportionality factor b (Eq.3 – 6) is unknown and only the relative spectral distributions to momentum flux and energy dissipation are available, assuming b is scale-independent. Momentum fluxes supported by larger wave scales fluctuate considerably between the four data sets. In all cases the momentum fluxes due to breaking waves is strongest at wave scales corresponding to phase speeds of about 6 – 9 ms^{-1}. At wave scales with $c < 5\,\mathrm{ms}^{-1}$ momentum fluxes supported by white capping waves falls off by roughly three orders of magnitude. Energy dissipation due to whitecaps is even more dominated by larger wave scales. The spectral distributions of the energy dissipation peak at c=8 – 10 ms^{-1} . Only in the case of the developing sea are dominant breakers involved in energy dissipation.

Breaking rate

The overall breaking rate R at a fixed location (Eq.2) is equivalent to the fractional surface area turnover rate at an arbitrary time. Thus, R is an important quantity for air-sea exchange processes, e.g. relevant for specifying surface renewal and bubble entrainment in air-sea gas flux models. It also provides insight to what conditions are favourable to wave breaking. Banner *et al.* (2002) found the breaking rate at specific scales to depend on some measure of the mean steepness, best expressed by the normalized saturation

$$\sigma(\omega) = \frac{\omega^5 S(\omega)}{2g^2 D(\omega)} \qquad (7)$$

where $D(\omega)$ is the angular spreading of the surface elevation spectrum. The breaking rate of different spectral bands ranging from the peak frequency ω_p up to $2.5\omega_p$ showed a clear threshold behaviour with breaking starting at a common saturation threshold of $\sigma \simeq 4.5\times10^{-3}$. This indirect breaking criterion is also verified by our current data. Saturation levels during data sets II and III are lower than for the two other data sets. Moreover, at lower frequencies, corresponding to waves with $c/c_p > 0.6$, saturation in II and III are below the threshold level (Figure 3) and no breaking occurred at these wave scales (Figure 2).

The overall breaking rate R includes contributions from all spectral wave scales. Therefore, we define the mean saturation level

$$\sigma_b = \left\langle \frac{\omega^5 S(\omega)}{2g^2 D(\omega)} \right\rangle \qquad (8)$$

where < > represents the average over the bandwidth $\omega_p \le \omega \le 5\omega_p$ and the duration of the data set.

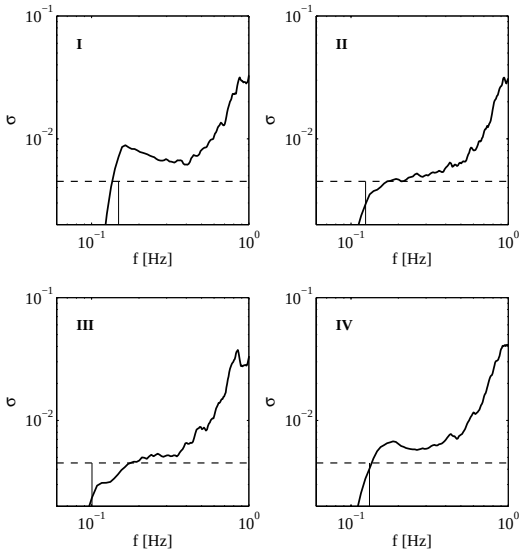

Figure 3: Wave saturation σ as function of frequency f (data sets as indicated in top right corner). The dashed horizontal line represents the threshold for onset of breaking as determined in Banner et al. (2002); the vertical line depicts the dominant wave frequency

Our observations cover the range of mean saturation levels $5.3\times10^{-3} \le \sigma_b \le 8.5\times10^{-3}$ (Figure 4). The breaking rate *R* ranges from roughly 50 to 120 breaking events per hour. Previous observations by various investigators using a wide range of observational techniques (for a summary see Gemmrich & Farmer, 1999) report breaking rates $R \simeq 0.1$ to $0.8 f_p$. For open ocean conditions these rates relate to the same range of values as observed in this study.

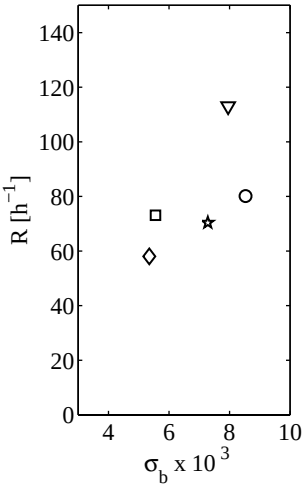

Figure 4: Breaking rate R as function of mean saturation level σ_b within the band $1 \le \omega/\omega_p \le 5$ and normalized by the theoretical spreading distribution. Symbols same as in Figure 2.

We find the breaking rate *R* to depend roughly linearly on the mean saturation level σ_b, with higher saturation levels leading to more frequent breaking. For this band averaged saturation the threshold for the onset of breaking, however, depends on the actual bandwidth chosen, and the absolute value is therefore somewhat arbitrary.

The good agreement in magnitude and functional dependency of breaking rates inferred from the breaking crest length distributions and various different observation techniques is encouraging that our analysis captures the majority of whitecap events.

Conclusions

The spectral scale and occurrence rate of breaking waves has been extracted from video recordings of the ocean surface. Most frequent wave breaking occurs at small to intermediate wave scales. The distribution of breaking

scales depends strongly on the wave field development. In fully developed seas the largest breakers have scales corresponding to half the dominant phase speed, whereas in developing seas breaking at the peak is observed. Wave breaking is the major mechanism of wave energy dissipation and a similar spectral shape and wave age dependence of the dissipation sink function are implied. A previous study found that the onset of breaking at any scale requires the wave saturation at this scale to be larger than a given threshold. This breaking threshold behaviour is confirmed with the present data set.

Acknowledgments: Many valuable discussions with Michael Banner and Chris Garrett helped to shape this work which is funded by the Canadian Foundation for Atmospheric and Climate Sciences (CFCAS).

References

Ardhuin, F., A.D. Jenkins, D. Hauser, A. Reniers and B. Chapron, Waves and operational oceanography: toward a coherent description of the upper ocean, *EOS., 86(4)*, 37, 40, 2005.

Banner, M.L., J.R. Gemmrich and D.M. Farmer, Multiscale measurements of ocean wave breaking probability, *J. Phys. Oceanogr., 32,* 3364 – 3375, 2002.

Ding, L. and D.M. Farmer, Observations of breaking surface wave statistics, *J. Phys. Oceanogr*. *24*, 1368-1387, 1994.

Duncan, J.D., An experimental investigation of breaking waves produced by an airfoil, *Proc. R. Soc, Lond. A*, *377*, 331-348, 1981.

Gemmrich, J.R. and D.M. Farmer, Near-surface turbulence in the presence of breaking waves, *J. Phys. Oceanogr*., *34*, 1067-1086, 2004.

Gemmrich, J.R. and D.M. Farmer, Observations of the scale and occurrence of breaking surface waves, *J. Phys. Oceanogr*., *29*, 2595-2606, 1999.

Melville, W.K. and P. Matusov, Distribution of breaking waves at the ocean surface. *Nature, 417,* 58-63, 2002.

Phillips, O.M., F.L. Posner and J.P. Hansen, High range resolution radar measurements of the speed distribution of breaking events in wind-generated ocean waves: Surface impulse and wave energy dissipation rates, *J. Phys. Oceanogr., 31*, 450-460, 2001.

Phillips, O.M., Spectral and statistical properties of the equilibrium range in wind-generated gravity waves, *J. Fluid Mech*., 156, *505-531,* 1985.